Investigation of isotopic dependence on the O + Ni fusion cross section near barrier energies

Nabendu Kumar Deb,[1] K. Kalita,[1,*] Harun Al Rashid,[1,2] Amar Das,[1,3] S. Nath,[4] J. Gehlot,[4] N. Madhavan,[4] Rohan Biswas,[4] Rudra N. Sahoo,[5] Pankaj K. Giri,[6,7] A. Parihari,[8] Niraj K. Rai,[9] Saumyajit Biswas,[10] Amritraj Mahato,[6] and B. J. Roy[11,12]

[1]*Department of Physics, Gauhati University, Guwahati 781014, Assam, India*
[2]*Department of Physics, BBK College, Nagaon, Barpeta 781311, Assam, India*
[3]*Department of Physics, Suren Das College, Hajo 781102, Assam, India*
[4]*Nuclear Physics Group, Inter-University Accelerator Centre, Aruna Asaf Ali Marg, New Delhi 110067, India*
[5]*Racah Institute of Physics, Hebrew University, Jerusalem 91904, Israel*
[6]*Department of Physics, Central University of Jharkhand, Ranchi 835205, Jharkhand, India*
[7]*Department of Physics, Chandigarh University, Mohali 140413, Punjab, India*
[8]*Department of Physics and Astrophysics, University of Delhi, Delhi 110007, India*
[9]*Department of Physics, Panjab University, Chandigarh 160014, Punjab, India*
[10]*Department of Physics, Murshidabad College of Engineering and Technology, Berhampore 742102, West Bengal, India*
[11]*Nuclear Physics Division, Bhabha Atomic Research Centre, Mumbai 400085, Maharashtra, India*
[12]*Homi Bhabha National Institute, Anushaktinagar, Mumbai 400094, Maharashtra, India*

(Received 8 December 2021; accepted 28 April 2022; published 19 May 2022)

Fusion excitation functions have been measured for $^{16}O + ^{61}Ni$ and $^{18}O + ^{61,62}Ni$ systems around the Coulomb barrier ($\approx 0.7V_B$–$1.3V_B$) using the recoil mass spectrometer, heavy ion reaction analyzer. The ground state Q value for two neutron stripping is positive for both systems with ^{18}O as the projectile. Strong enhancement of the experimental fusion cross sections were observed below the barrier for all the systems compared to that of the predictions of the one-dimensional barrier penetration model. To understand such enhancement, a coupled-channels formalism has been used. A comparative study of these systems indicated that the coupling of two neutron transfer channels with the collective excitations could play the role behind the sub-barrier fusion enhancement for ^{18}O induced reactions. However, the sub-barrier enhancement for $^{16}O + ^{61}Ni$ is found to be due to the coupling of quadrupole vibrations of both the interacting nuclei. Also after comparing these systems with other systems of different Ni isotopes, we have found that the signature of the role of coupling to neutron transfer channels due to ground state positive Q value for neutron transfer is ambiguous.

DOI: 10.1103/PhysRevC.105.054608

I. INTRODUCTION

Enhancement in the sub-barrier fusion cross section, in comparison with the predictions of the one-dimensional barrier penetration model (1DBPM), is observed for many systems in the last few decades, owing to the advent of many experimental facilities and techniques [1–3]. The reason ascribed for such enhancement is the coupling of various intrinsic degrees of freedom which governs the fusion dynamics near the Coulomb barrier (V_B) [4–6]. Such couplings like relative motion to the degree of freedom associated with inelastic collective excitations and nucleon transfers modifies the tunneling process vigorously, thereby leading to broadening of spin distributions of compound nuclei, splitting of single barrier into manifold barrier, etc. In the coupled channel (CC) framework, coupling to the inelastic excitations in near barrier is well described [7,8]. Such CC calculations could reproduce the experimental data correctly for most of the systems. However, there are many experimental proofs which attribute the neutron transfer with positive Q values for the additional observed enhancement of the sub-barrier fusion cross section, as such enhancement could not be reproduced by CC calculations without considering neutron transfer [9–12]. Contrary to these observations, there are certain systems in which the role of positive Q value neutron transfer channels is found to be negligible in the sub-barrier fusion [13,14]. Such ambiguity in observations indicates the importance of describing the sub-barrier fusion enhancement in terms of the coupling of neutron transfer channels. The theoretical model correctly predicting such enhancement due to neutron transfer is yet to be made available.

The possible transfer reaction influence was observed on the sub-barrier cross sections of Ni + Ni fusion reactions [15]. Following this study, many experiments were performed on different systems, especially the systems having positive ground state Q value neutron transfer channels as they would give rise to a barrier in the lower energy regime compared to that of inelastic couplings [16], and an effort has also been made to separate the few nucleons transfer effect on the fusion process.

*ku_kalita@yahoo.com

A case study done for $^{40}Ca + ^{90,96}Zr$ systems displayed strongly the interplay of collectivity, transfer in fusion enhancement [17]. A strong isotopic dependence is observed in these systems where ^{96}Zr was found to have more enhancement than ^{90}Zr at the sub-barrier region. This extra enhancement was due to the transfer channel coupling as for the $^{40}Ca + ^{96}Zr$ system, the Q value is positive for up to eight neutron transfer while for ^{90}Zr the Q value is negative for all transfer channels. However, in another study with the same systems, it was observed that the 3^- state is stronger in the case of ^{96}Zr than that of ^{90}Zr which could play an important role in the fusion enhancement rather than the positive Q value neutron transfer channel effect [18]. Investigations were also done on the claimed effect of the 3^- state of ^{96}Zr in the systems $^{36}S + ^{90,96}Zr$ [19] having large negative Q values for all neutron transfer. The results indicated the strong coupling of the 3^- vibration of ^{96}Zr behind the cross section enhancement. Similar attempts were made to study the effect of transfer channel couplings on different systems such as $^{40}Ca + ^{46,48,50}Ti$; $^{32,36}S + ^{94,96,98,100}Mo$, $^{100,101,102,104}Ru$, $^{104\text{–}106,108,110}Pd$; $^{40}Ca + ^{40,44,48}Ca$; $^{40,48}Ca + ^{90,94,96}Zr$; $^{32}S + ^{94,96}Zr$; $^{28}Si + ^{90,92,94}Zr$; $^{28}Si + ^{142,150}Zr$; $^{35,37}Cl + ^{130}Te$; $^{16}O + ^{58,62}Ni$; $^{18}O + ^{112,116}Sn$; $^{58}Ni + ^{58,64}Ni$ and $^{32,36}S + ^{58,64}Ni$ [4,5,17,20–33]. Strong isotopic dependences were observed in these systems where the different isotopes considered as the target in each case have similar collective strengths, due to which the experimental signature of transfer channels could be highlighted. The isotopic differences of fusion enhancements suggest the significance of involvement of the transfer channels in the computation [34]. Thus to extricate the role of neutron transfer coupling and the effect of collective excitations behind the sub-barrier fusion enhancement, the systems should possess weak or similar inelastic excitations.

In the present work, the fusion excitation functions were measured for $^{16}O + ^{61}Ni$ and $^{18}O + ^{61,62}Ni$ system, with the ^{18}O-induced systems having positive ground state Q values for the two neutron transfer channel whereas $^{16}O + ^{61}Ni$ system have negative Q values for all the neutron transfer channels, thereby searching for the fact that the neutron transfer channel could play a role in the sub-barrier fusion cross sections. ^{16}O is spherical and the deformation effect of ^{18}O is minimal [35]. The Ni isotopes, considered in our work, are nearly spherical having similar shell structures with the lowest quadrupole and octupole states being collective in nature with similar collective strengths. The deformation values or the energy levels of the different isotopes do not possess any considerable differences. Therefore, strong isotopic dependence is not expected considering collective excitations of the target nuclei. Nevertheless due to coupling to positive Q value neutron transfer channels, the present measurement allows us to study the isotopic dependence of the fusion excitation function for these systems. Table I shows the ground state Q values of different systems for the various transfer channels. It, thus, offers the chances of examining the multineutron transfer effects on the fusion process. Moreover in the case of the odd ^{61}Ni isotope, the analog of first collective state 2^+ in even Ni isotopes is split into a multiplet. In the calculations, the multiplet was introduced as a single effective state given as a spin average of the four states [36,37]. The effective energy and the corresponding deformation parameters of the multiplet is calculated using the formula discussed in Ref. [38]. We will also examine the effect of coupling of single and multiphonon states on the sub-barrier fusion process in the framework of the CC formalism. The paper presents the experimental setup in Sec. II followed by the description of data reduction techniques and the details of its analyses within the CC model in Sec. III. Section IV gives the summary of the work done and the conclusion.

TABLE I. The Q values (in MeV) for the neutron transfer of the different systems. "Q''_{-xn} refers to ground state Q values for stripping reaction where x number of neutrons transferred from projectile to target whereas "Q''_{+xn} refers pickup reactions.

Reactions	Q_{-3n}	Q_{-2n}	Q_{-1n}	Q_{+1n}	Q_{+2n}
$^{16}O+^{61}Ni$	−24.975	−11.453	−5.068	−3.677	−7.019
$^{18}O+^{61}Ni$	−0.761	5.245	2.550	−3.864	−7.644
$^{18}O+^{62}Ni$	−5.259	4.307	−1.208	−6.640	−6.852

II. EXPERIMENTAL SETUP

The fusion cross sections have been measured using both ^{16}O and ^{18}O as pulse beams, with 4 μs pulse separation, provided by the 15UD Pelletron accelerator facility at the Inter-University Accelerator Center (IUAC), New Delhi [39], with methodology being similar to that of Ref. [32]. The targets used for this work were ^{61}Ni (99.39% enriched) and ^{62}Ni (98.45% enriched), having thicknesses of 106 $\mu g/cm^2$ and 156 $\mu g/cm^2$, respectively, prepared on carbon backings of approximately 30 $\mu g/cm^2$ thickness using a physical vapor deposition technique [40,41]. The targets were kept in such a way that the carbon faces the beam. The measurements were done using the recoil mass spectrometer, the heavy ion reaction analyzer (HIRA) [42] at the laboratory energy (E_{lab}) range of 34.6 MeV to 49.7 MeV (covering 12.7% below the barrier to 25.3% above the barrier) for $^{16}O + ^{61}Ni$, 33.6 MeV to 52.6 MeV (covering 16.4% below the barrier to 31.1% above the barrier) for $^{18}O + ^{61}Ni$ and 33.9 MeV to 52.9 MeV (covering 15.2% below the barrier to 32.1% above the barrier) for $^{18}O + ^{62}Ni$ systems. In this energy range, the contribution due to fission is found to be negligible [43]. Hence the fusion yield is the sum of the total yield of the evaporation residues (ER) which gives the fusion cross section. ERs were detected at the focal plane of HIRA by a multiwire proportional counter (MWPC) of active area 150 × 50 mm^2 operated at a pressure of 3 mbar isobutene gas. ERs are dispersed at the focal plane of the HIRA according to their mass to charge (A/q) ratio and the intense beam background is rejected. The time of flight (TOF) was obtained from a time-to-amplitude converter (TAC) with the start signal from the focal plane detector and the stop signal as delayed radiofrequency from the beam pulsing system. Due to this TOF measurement, a clean separation between the beamlike particles and the ERs can be seen as shown in Fig. 1 which allowed us to measure fusion cross section (σ) down to $E_{lab} \approx 34$ MeV for these three systems.

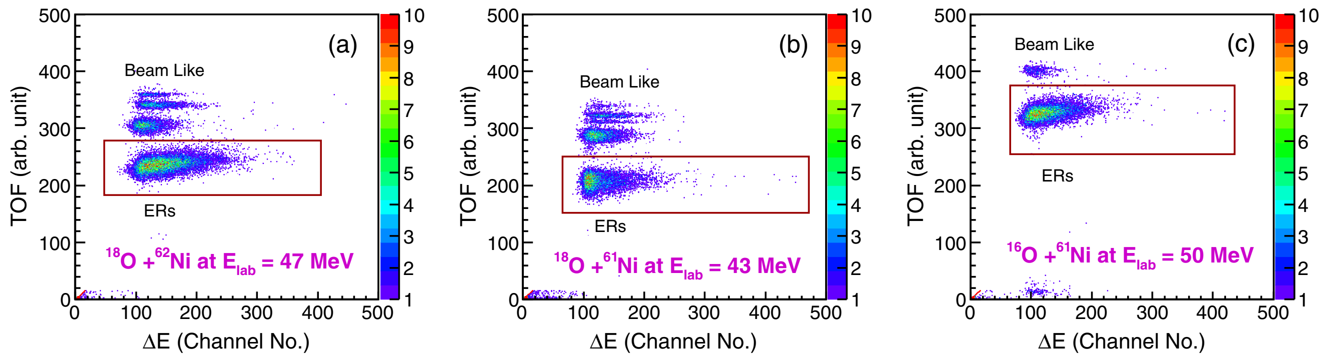

FIG. 1. Two-dimensional ΔE-TOF spectra obtained for (a) the $^{18}O + ^{62}Ni$ system at $E_{\mathrm{lab}} = 47$ MeV; (b) the $^{18}O + ^{61}Ni$ system at $E_{\mathrm{lab}} = 43$ MeV; and (c) the $^{16}O + ^{61}Ni$ system at $E_{\mathrm{lab}} = 50$ MeV, shown here as representative cases. The groups of ERs and the beam-like particles are well separated from each other. The rectangles enclosing the ERs at different energies were used to account for the fusion events. Both x and y axes are displayed in arbitrary units (channel numbers).

Figure 2 shows the spectra for these three systems corresponding to the lowest possible energy in the laboratory frame where ER counts could be obtained. The ER yield so obtained within the gate marked in each of the spectrums is very low. Inside the target chamber, two silicon-surface barrier detectors (SSBD) were mounted symmetrically at 15.5° in the horizontal plane to monitor the beam direction and for normalization of cross sections during data analysis. A carbon foil of ≈30 μg/cm^2 thickness was mounted 10 cm downstream from the target to reset the ER charge state to equilibrium distribution, following internal conversion, if any. Data were collected in event mode using FREEDOM [44] and offline analyses were done using CANDLE [45] and ROOT [46] softwares.

III. DATA ANALYSIS AND RESULTS

The fusion cross sections were obtained at different energies using the standard procedure discussed in Refs. [47,48]. The set of fusion cross sections so obtained for $^{16}O + ^{61}Ni$ and $^{18}O + ^{61,62}Ni$ systems and the corresponding uncertainties are reported in Table II and are shown in Figs. 3–5. The uncertainties quoted in the fusion cross section are the absolute errors that include the statistical errors due to the total number of events detected in the focal plane detector of HIRA, the error involved in the derived quantities which is calculated using the standard error propagation formula, the error due to the uncertainty in the measurement of the detector solid angles, and the error in HIRA efficiency. The lesser ER statistics is one of the reasons for significant error in the last two data points for $^{18}O + ^{61,62}Ni$ systems.

Among all these quantities, the transmission efficiency of HIRA (ε) contributes the maximum in overall error in the final cross sections (≈0.1 in the simulated value with respect to the measured efficiency) in different systems corresponding to all the data points [47,49]. ε is a complex function of several reaction-specific and instrument-specific parameters, viz., entrance channel mass asymmetry, beam energy, target thickness, exit channel of interest, angular acceptances of particles of interest and the HIRA, reference particle settings of HIRA, size of the focal plane detector [49]. It is defined by the ratio of the number of ERs reaching the HIRA focal plane to the total number of ERs emerging from the target. Although the entrance channel mass asymmetry, target thickness, HIRA angular acceptance, and focal plane detector size remains fixed throughout, the other parameters change. Thus ε would be different for each energy in the laboratory frame (E_{lab}). Besides, several ER channels are populated at a particular E_{lab}. The HIRA is normally set for the most dominant ER channel, thereby transmitting ERs from different channels with different ε. As measuring ε for each exit channel at each E_{lab}

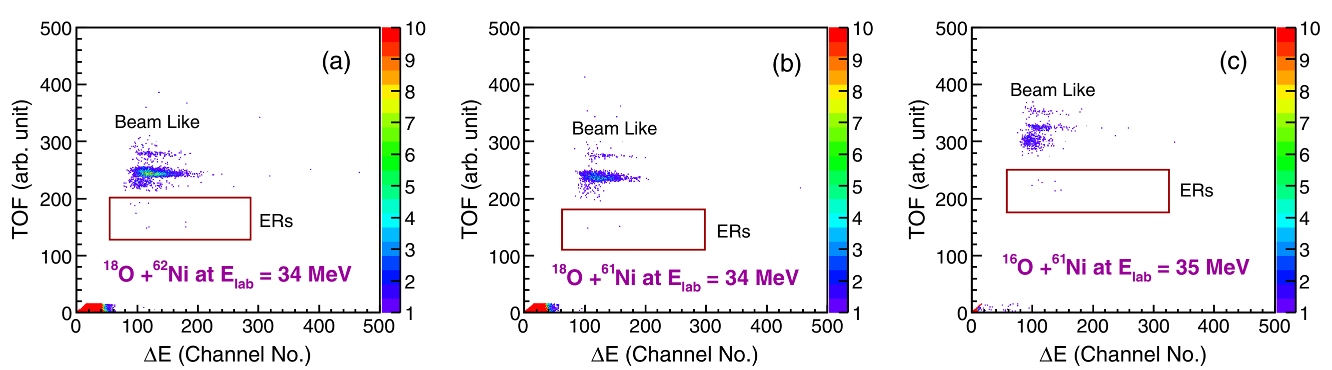

FIG. 2. Same as in Fig. 1 but for (a) the $^{18}O + ^{62}Ni$ system at $E_{\mathrm{lab}} = 34$ MeV; (b) the $^{18}O + ^{61}Ni$ system at $E_{\mathrm{lab}} = 34$ MeV; and (c) the $^{16}O + ^{61}Ni$ system at $E_{\mathrm{lab}} = 35$ MeV, which corresponds to the lowest energy of the measured cross section for each system.

TABLE II. Fusion cross sections (σ) measured experimentally for $^{18}O + ^{61,62}Ni$, $^{16}O + ^{61}Ni$ systems at energies ($E_{c.m.}$) in the center-of-mass frame with the corresponding errors in cross sections ($\delta\sigma$).

$^{18}O + ^{61}Ni$		$^{18}O + ^{62}Ni$	
$E_{c.m.}$ (MeV)	$\sigma \pm \delta\sigma$ (mb)	$E_{c.m.}$ (MeV)	$\sigma \pm \delta\sigma$ (mb)
25.9	0.069 ± 0.049	26.3	0.076 ± 0.041
26.3	0.142 ± 0.069	26.7	0.131 ± 0.056
27.5	0.631 ± 0.169	27.9	0.776 ± 0.211
28.6	2.43 ± 0.49	29.1	3.61 ± 0.726
29.4	6.80 ± 1.36	29.8	12.1 ± 1.88
30.2	22.4 ± 3.29	30.6	29.8 ± 4.00
30.6	40.9 ± 4.83	31.4	66.2 ± 9.01
30.9	56.0 ± 9.02	31.8	105 ± 12.3
31.3	105 ± 12.3	32.5	161 ± 18.8
32.1	159 ± 18.3	33.3	202 ± 23.5
32.9	213 ± 27.8	34.9	294 ± 33.2
34.4	328 ± 36.7	36.4	418 ± 49.1
36.0	443 ± 52.3	37.9	500 ± 61.4
37.5	545 ± 67.1	39.5	617 ± 74.4
39.1	633 ± 77.0	41.1	774 ± 98.6
40.6	813 ± 98.9		

$^{16}O + ^{61}Ni$	
$E_{c.m.}$ (MeV)	$\sigma \pm \delta\sigma$ (mb)
27.3	0.077 ± 0.037
28.2	0.380 ± 0.087
29.0	1.71 ± 0.33
30.6	24.2 ± 3.23
32.2	120 ± 14.4
34.6	288 ± 33.3
37.0	470 ± 54.5
39.4	601 ± 71.3

was not possible practically, we relied on the semimicroscopic Monte Carlo code, TERS [50] for the precise estimation of the ε theoretically. This code simulates HIRA and gives absolute transmission efficiency for a system. The relative population

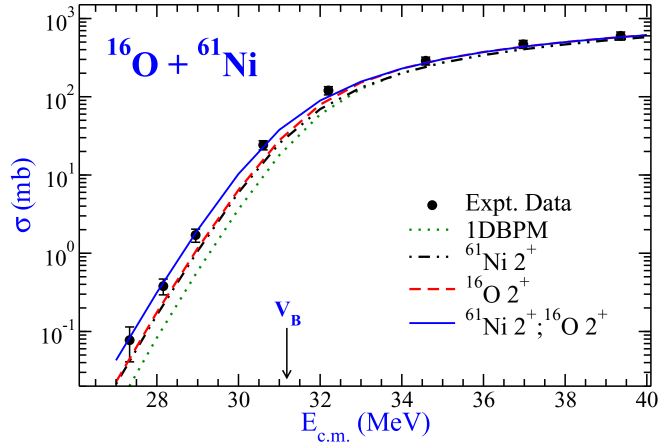

FIG. 3. Experimental fusion excitation function for the $^{16}O + ^{61}Ni$ system along with results of the calculation involving different modes of coupling between interacting partners using the CCFULL code.

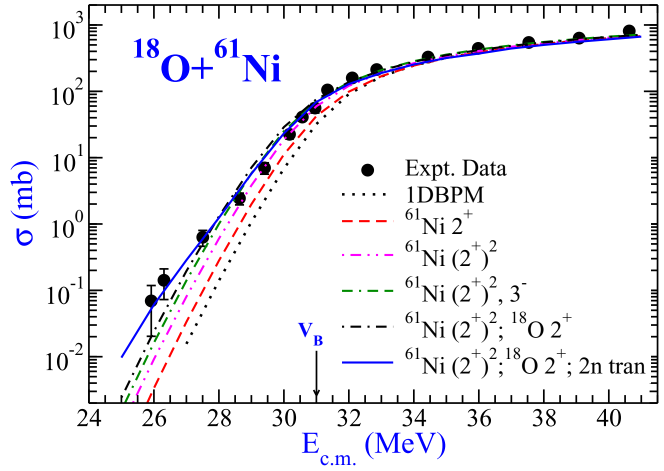

FIG. 4. Same as in Fig. 3 but for the $^{18}O + ^{61}Ni$ system.

of different ER channels in the present systems was estimated by the statistical model code PACE4 [43].

The energies quoted in Table II are corrected for the corresponding energy loss in the carbon backing of the target and the half-target thickness. From the figures, it can be seen that the sub-barrier cross sections for these three systems are enhanced as compared to the 1DBPM. In order to understand these observations further, the CC formalism CCFULL [51] is employed. The CCFULL calculations were carried out using Wood-Saxon parametrizations of the Akyüz-Winther (AW) potential [52,53]. The nuclear potential parameters so calculated for these systems are listed in Table III. The potential parameters are considered here in such a way that they fit the fusion cross sections above the Coulomb barrier and give equivalent barrier parameters which is also quoted in Table III. The deformation and the energy values of the low-lying states for the various nuclei [12,54], obtained using the expression given in Ref. [4], are enumerated in Table IV. The case of ^{61}Ni is somewhat more complicated as it is an odd-A nucleus whose ground state spin is not 0 and unlike as in $^{60,62}Ni$ nuclei, there is no single 2^+ level in an excited state of ^{61}Ni. Instead,

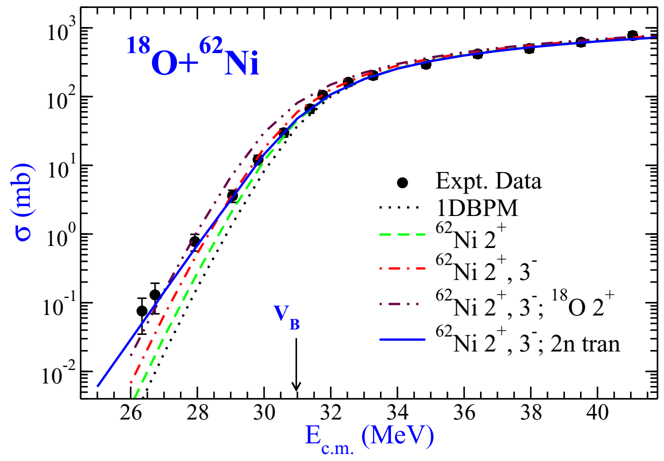

FIG. 5. Same as in Fig. 3 but for the $^{18}O + ^{62}Ni$ system.

TABLE III. Woods-Saxon parameters of the AW potential used in our CC calculations for different systems.

Reactions	V_0 (MeV)	r_0 (fm)	a (fm)	V_B (MeV)	R_B (fm)	$\hbar\omega$ (MeV)
$^{16}O+^{61}Ni$	77	1.14	0.62	31.60	9.53	3.90
$^{18}O+^{61}Ni$	83	1.13	0.63	31.13	9.67	3.65
$^{18}O+^{62}Ni$	80	1.13	0.64	31.01	9.70	3.60

there is a multiplet of states corresponding to the one phonon 2^+ and 3^- states in ^{60}Ni. In the weak coupling approximation, the multiplet is formed by the coupling of the single phonon state in ^{60}Ni with the valence neutron in the $2p_{3/2}$ orbit, which can be replaced by a single effective state given by the spin average of the multiplet states [36]. Using this method, the energy was calculated well but the β_2 value was largely underestimated as the relation between an experimental $B(E2)$ and β_2 is not the same as that for a transition from the 0^+ ground state to the 2^+ state in even-even nuclei [38]. Thus, the prescription described in Ref. [55] is adopted to determine the β_2 value for the effective collective state in ^{61}Ni which is found out to be 0.24. These spectroscopic properties of the interacting partners were incorporated in the CC calculations without changing the potential parameters. The calculations are then compared with the fusion excitation function as CCFULL can include all orders of couplings. As for the inelastic channels, all known states with a significant $E2$ or $E3$ transition strength to the ground state were taken into account. The code CCFULL can also schematically take into account the effect of a nucleon pair-transfer channel using a macroscopic form factor for the coupling strength, which, along with the Q value for the neutron pair-transfer channel are considered as free parameters to obtain the best agreement between the experimental and theoretical fusion excitation functions.

The fusion excitation function along with the CC calculations for $^{16}O+^{61}Ni$ is shown in Fig. 3. CC calculations were carried out with both ^{16}O and ^{61}Ni as vibrators. From the figure, it is seen that by considering the single phonon 2^+ or 3^- vibrational states of ^{61}Ni or 2^+ states of ^{16}O individually, we could not reproduce the experimental data, although they have shown slight enhancement compared to that of 1DBPM. It was observed that the 3^- state of the ^{16}O nucleus, although it is more collective, overestimates the experimental fusion cross sections significantly. But considering the coupling scheme of the single phonon 2^+ vibrational state of ^{61}Ni with that of the 2^+ vibrational state of ^{16}O, the experimental data could be reproduced quite well. When we consider the coupling with neutron transfer, the result is enhanced compared to the experimental sub-barrier fusion cross sections, which is quite expected as the system do not possess positive Q values for the neutron transfer channels, hence is not shown in the figure.

The fusion excitation function along with the CC calculations for $^{18}O+^{61}Ni$ is shown in Fig. 4 which were carried out with both ^{18}O and ^{61}Ni as vibrators. From Fig. 4 it is seen that by considering the single phonon or double phonon 2^+ vibrational states of ^{61}Ni or mutual coupling of 2^+ and 3^- vibrational states of ^{61}Ni, we could not reproduce the experimental data. The various single channel coupling modes of projectile and target excitations have meagre effects in the sub-barrier region compared to that of 1DBPM hence is not shown here. Eventually excitations of single phonon vibrational states of ^{18}O were also included in the coupling scheme along with the double phonon 2^+ vibrational states of ^{61}Ni. In the calculation, the two phonon excitations in the harmonic oscillator approximation have been included. The energy of the two phonon state, in this case, is taken to be twice that of the one phonon and the deformation value is the square root of the quadratic sum of the deformation parameters of the single phonon states [16]. Yet they could not reproduce the data satisfactorily. But when the coupling of a pair of neutron transfer is taken into account in the CC calculations for this system with transfer form factor being 0.45 MeV, the experimental data could be reproduced quite well. This CC analysis including the couplings of the neutron transfer channels has been carried out in order to investigate whether or not the sub-barrier fusion enhancement for this system could be explained in terms of neutron transfer channels. In CC calculations, the inclusion of transfer coupling requires a transfer form factor derived from the experimentally measured transfer probability. As the transfer cross sections have not been measured for the present system, CC calculations were carried out with various values of transfer form factor. With 0.45 MeV value, CC calculations provided an improved description of experimental fusion cross sections at sub-barrier energies within the experimental uncertainties. From this analysis, we could infer that the positive Q-value neutron transfer channels should be taken into account while interpreting the sub-barrier fusion enhancement of this system. To validate such a calculation and to see if the relevant neutron transfer cross section is consistent with the value of the coupling strength assumed here, the inclusive measurement of fusion along with the different transfer measurements should be carried out.

In Fig. 5, similar CC calculations were carried out with another isotope ^{62}Ni which is also considered as a vibrator. Even in this system, single channel coupling due to both the

TABLE IV. Deformation parameters (β) and excitation energies (E_λ) along with the ground state spectroscopic properties of ^{16,18}O and ^{61,62}Ni nuclei used in the CC calculations [12,55].

Nucleus	λ^π	E_λ (MeV)	β_λ
^{16}O	2^+	6.917	0.362
	3^-	6.129	0.79
^{18}O	2^+	1.982	0.355
	3^-	5.098	0.39
^{61}Ni	2^+	0.964	0.24
	3^-	3.9	0.20
^{62}Ni	2^+	1.17	0.21
	3^-	3.75	0.22

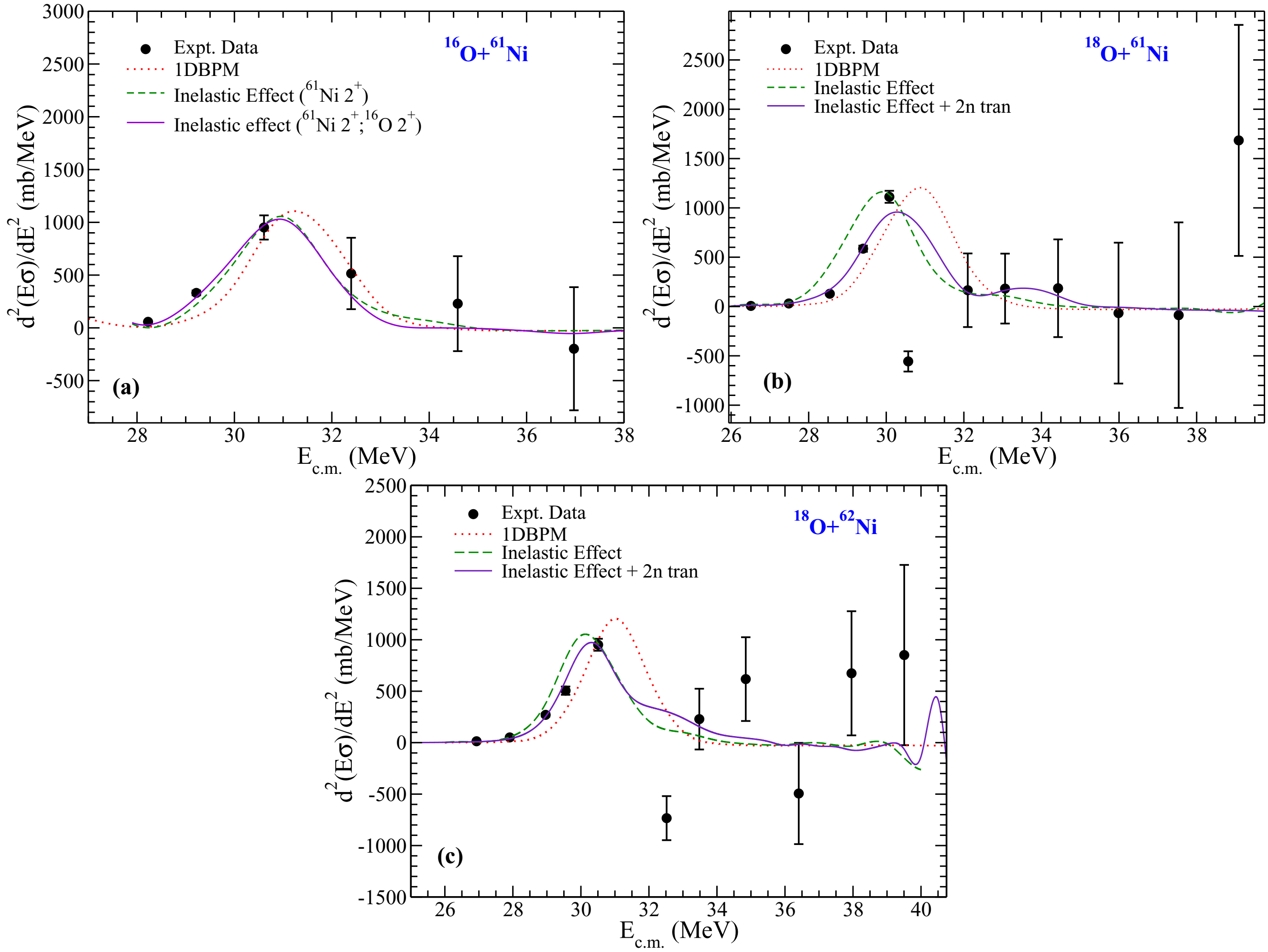

FIG. 6. The fusion barrier distribution for (a) the $^{16}O + ^{61}Ni$, (b) the $^{18}O + ^{61}Ni$, and (c) the $^{18}O + ^{62}Ni$ systems. Lines and curves are self-explanatory.

projectile (^{18}O) and the target excitations could not reproduce the data satisfactorily. Also, considering the mutual coupling scheme of multiphonon vibrational states of the target with the single 2^+ excited state of the projectile, the experimental data could not be reproduced in the barrier and the sub-barrier energies. When the neutron transfer is considered in this system along with the mutual coupling scheme of multiphonon vibrational states of the target and with coupling strength of 0.3 MeV, the experimental data are reproduced fairly well.

Figure 6 shows the barrier distribution (BD) curve for the present systems. The BD is related to the second derivative of the fusion cross section. The BD was extracted using the point difference formula [48,56,57]. As can be seen in the figure, BD is well defined towards the lower energies, but it shows large fluctuations towards higher energies. To reduce errors at the higher energies, small energy steps are required, but in this work a larger step size of the energy is considered. The measured distributions were shown with that of the 1DBPM calculation using the parameters quoted in Table III. It shows a single broad peak shifted towards lower energies compared to 1DBPM barrier peak for these three systems, i.e., the maximum is obtained at energy below the nominal Coulomb barrier. The measured peak of $^{18}O + ^{61}Ni$ is somewhat reproduced by considering two neutron transfer coupling. Even $^{18}O + ^{62}Ni$ shows the similar result supporting the neutron transfer channel for these systems to an extent. But for $^{16}O + ^{61}Ni$, the inelastic excitation considering the single phonon 2^+ vibrational state of ^{61}Ni with that of the 2^+ vibrational state of ^{16}O is found to be enough to match the experimental BD in the lower energy regime. But overall, the BDs obtained here are very ill defined and show no discrimination between the two ^{18}O-induced systems. To have proper shape of BD, more precise data at smaller intervals are obviously needed compared to what we have at hand. Moreover the target thickness considered in this work was clearly not suitable for BD measurement. Consequently, it was not possible to draw proper conclusions from BDs independently. Hence, the inference from BD on the role played by the transfer coupling channel seems elusive in this case.

After knowing the probable reason for sub-barrier enhancement, comparisons were made among these three systems to understand the isotopic dependence. A general

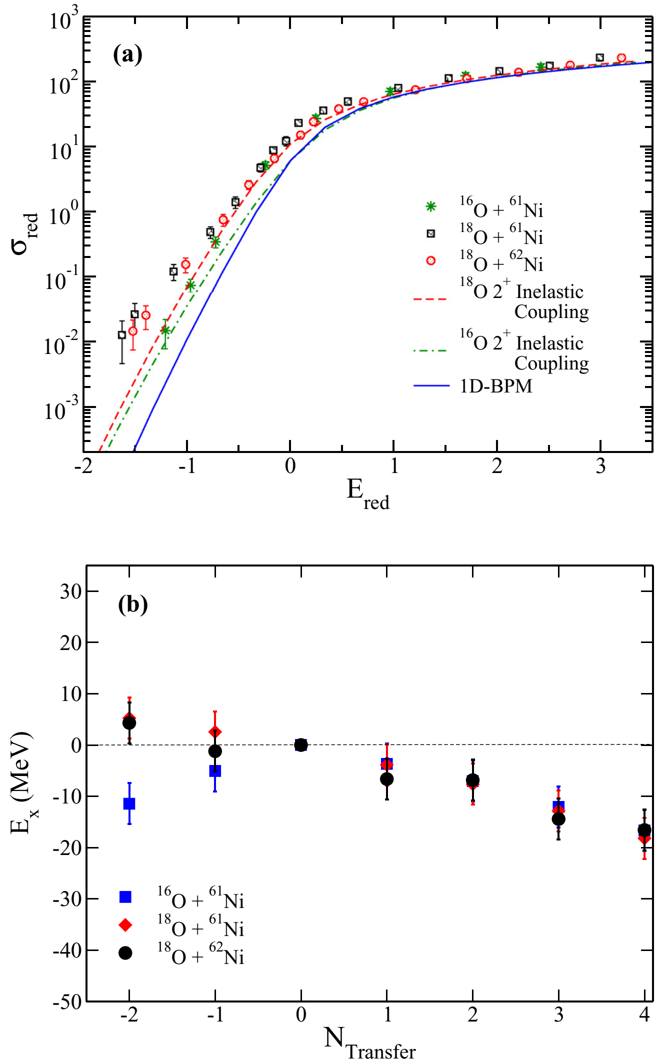

FIG. 7. (a) The measured fusion cross sections in reduced scales and (b) the average excitation energies (E_x) of the residual nuclei following neutron transfer (N_{Transfer}). Lines and curves are self-explanatory. Refer to text for more details.

isotopic effect in fusion reactions has been studied for many years but is still being debated on the different enhancement observed for the fusing systems with same Coulomb factor (Z_pZ_t), where Z_p, Z_t are the atomic numbers of the projectile and target, respectively, but different masses, i.e., A_pA_t, where the couplings of transfer reactions to the fusion channel play an important role [58]. The systems considered in this work have similar Z_pZ_t values and have both positive and negative ground state Q values for the particular neutron transfer channels which makes comparison quite effective. To enable the straightforward comparisons, reduced data is discussed in Fig. 7. In order to explore the role of neutron transfer between the interacting nuclei in the fusion process, the reduced fusion function of the present system has been plotted in Fig. 7(a). Here, σ_{red} and E_{red} are the dimensionless fusion function and the dimensionless variable defined as in Refs. [4,12]. The necessary barrier parameters required for the fusion function has been obtained from the CCFULL program. From Fig. 7(a), it can be seen that the isotopic effect is very much prevalent indicating that the coupling to two neutron channel is effective for the two ^{18}O-induced systems and hence are expected to play the role behind the sub-barrier fusion enhancement compared to that of 1DBPM cross section. Thus there are isotopic differences in the effects of the couplings. In the same figure, the CCFULL cross sections with inelastic couplings to the 2^+ vibrational states of both ^{16,18}O projectiles has been included. There we can see that the low lying 2^+ state of ^{18}O is more effective in enhancing the sub-barrier cross section compared to that of ^{16}O nucleus.

It was discussed that at energies around the Coulomb barrier, heavy-ion induced transfer reactions follow the Q-value systematics [54]. It predicts that in the outgoing channel, the preferred states are the ones located inside a Gaussian-shaped Q distribution with its centroid at the optimum Q value (Q_{opt}) given by

$$Q_{opt} = Q - E_x = E_{\text{c.m.}}\left(\frac{V_{B_f}}{V_{B_i}} - 1\right),$$

where Q and E_x is the ground state Q value and the excitation energy in the outgoing channel, respectively; $E_{\text{c.m.}}$ and $V_{B_{i,f}}$ is the energy in center of mass frame and the Coulomb barrier energies in the entrance or exit channels respectively. Using this relation, following the prescription discussed in Ref. [54], the excitation energies, E_x in MeV, resulting from the one to four neutron pickup and one to two neutron stripping (N_{Transfer}) has been calculated for the present systems as shown in Fig. 7(b). In the horizontal axis of the figure, N_{Transfer} is negative for neutron stripping and positive for neutron pickup accordingly. As can be seen from the figure, positive excitation energies and hence larger transfer yields are expected for the $^{18}\text{O} + {}^{61,62}\text{Ni}$ systems. These systems also exhibit shallower slopes in the fusion excitation functions (Fig. 7(a)).

Further comparisons were made with similar systems of various isotopes having similar Z_pZ_t [5,59,60]. To nullify the barrier parameters of different systems, the reduced cross section is plotted in Fig. 8, where the scaling of σ and $E_{\text{c.m.}}$ was done using the geometrical cross sections (πR_B^2) and the barrier heights (V_B), respectively. A marked isotopic effect is observed between the systems induced by ^{16}O and that of ^{18}O. These ^{18}O induced systems seem to display enhanced cross sections compared to that of ^{16}O induced reactions. In that case, the effect could be due to the neutron transfer for the systems with projectile ^{18}O as these systems possess a positive ground state Q value corresponding to two neutron transfer channel. The importance of coupling to transfer channels cannot, though, be inferred unambiguously in these systems. For $^{16}\text{O} + {}^{60,64}\text{Ni}$ systems, data are not available below the Coulomb barrier. More data are required for these systems to figure out the behavior of the sub-barrier fusion cross section although they do not possess positive Q values for the neutron transfer channel. To understand all these systems further, fusion data below the Coulomb barrier are called for to see the effects of single and multineutron transfer. In order to find out whether other systems also exhibit similar behavior, in this figure, $^{16,18}\text{O} + {}^{74,76}\text{Ge}$ [14] has been plotted

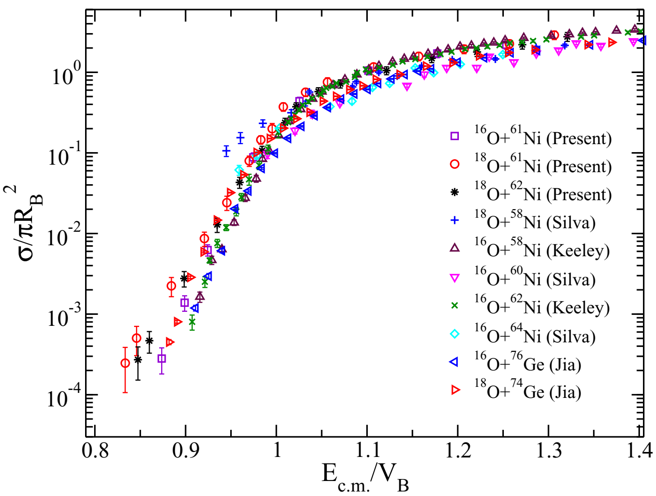

FIG. 8. Reduced fusion excitation functions of various systems with similar Coulomb factor for comparisons. Refer to text for details.

for comparative studies as the Z_pZ_t value of these systems is close to the O + Ni systems. Enhancement for both these systems in the sub-barrier regions are also visible. But, when the reanalysis of the $^{18}\mathrm{O} + {}^{74}\mathrm{Ge}$ system having positive Q value neutron transfer channel was carried out within our analysis framework, it was observed that there is no role of neutron transfer in the sub-barrier fusion of the $^{18}\mathrm{O} + {}^{74}\mathrm{Ge}$ system. There is no additional fusion enhancement at the sub-barrier energies for the $^{18}\mathrm{O} + {}^{74}\mathrm{Ge}$ system compared to the $^{16}\mathrm{O} + {}^{76}\mathrm{Ge}$ system despite the former reaction having positive Q value for the two neutron stripping channel. Both the reactions could be well interpreted by couplings to the low-lying excitation states. Thus the proper inference on the role of neutron transfer on the sub-barrier fusion enhancement still remains an open challenge.

IV. SUMMARY AND CONCLUSIONS

Fusion cross section measurements were carried out for $^{16}\mathrm{O} + {}^{61}\mathrm{Ni}$ and $^{18}\mathrm{O} + {}^{61,62}\mathrm{Ni}$ systems in energies ranging from $\approx 0.7V_B$–$1.3V_B$ for all these systems using the recoil mass spectrometer, HIRA. The fusion excitation functions and the barrier distributions so obtained for $^{18}\mathrm{O} + {}^{61,62}\mathrm{Ni}$ systems could be explained by including the two neutron transfer channel in the CC calculations but for $^{16}\mathrm{O} + {}^{61}\mathrm{Ni}$ system, simply coupling with the single phonon 2^+ vibrational state of $^{61}\mathrm{Ni}$ with that of the 2^+ vibrational state of $^{16}\mathrm{O}$, the experimental data could be reproduced quite well. As expected, strong isotopic dependences were observed between these systems and hence it could be inferred that the coupling effects including the transfer channel due to $^{18}\mathrm{O}$ on both $^{61}\mathrm{Ni}$ and $^{62}\mathrm{Ni}$ isotopes are similar and is quite different from that of the $^{16}\mathrm{O} + {}^{61}\mathrm{Ni}$ system. But when the $^{18}\mathrm{O}$-induced systems were compared with the other $^{16}\mathrm{O}$-induced systems with different Ni isotopes, isotopic dependence was observed to an extent. This observation revealed the $^{18}\mathrm{O}$-induced systems showing additional enhancement which could be basically due to neutron transfer channels with large positive Q value for these systems. Again, on comparing $^{18}\mathrm{O} + {}^{74}\mathrm{Ge}$ with $^{16}\mathrm{O} + {}^{76}\mathrm{Ge}$, it is observed that the sub-barrier fusion enhancement of the former system does not follow the trend. Thus more such data are required to improve the CC theory and other theoretical models.

ACKNOWLEDGMENTS

The authors are extremely grateful to the IUAC Pelletron staff for providing a stable beam and the target development laboratory group of IUAC for fabrication of thin enriched targets of good quality. One of the authors (N.K.D.) acknowledges the Council of Scientific and Industrial Research (CSIR), New Delhi for the JRF award of Grant no. 09/059(0056)/2014–EMR–I. The authors would like to acknowledge the help received from Ms. Anjali Rani, Delhi University and Mr. A. Vinayak, Karnatak University, during the experiment.

[1] G. Montagnoli and A. M. Stefanini, Eur. Phys. J. A **53**, 169 (2017).

[2] J. D. Bierman, P. Chan, J. F. Liang, M. P. Kelly, A. A. Sonzogni, and R. Vandenbosch, Phys. Rev. Lett. **76**, 1587 (1996).

[3] J. F. Liang, D. Shapira, C. J. Gross, J. R. Beene, J. D. Bierman, A. Galindo-Uribarri, J. G. delCampo, P. A. Hausladen, Y. Larochelle, W. Loveland, P. E. Mueller, D. Peterson, D. C. Radfrod, D. W. Stracener, and R. L. Varner, Phys. Rev. Lett. **91**, 152701 (2003).

[4] S. Kalkal, S. Mandal, N. Madhavan, E. Prasad, S. Verma, A. Jhingan, R. Sandal, S. Nath, J. Gehlot, B. R. Behera, M. Saxena, S. Goyal, D. Siwal, R. Garg, U. D. Pramanik, S. Kumar, T. Varughese, K. S. Golda, S. Muralithar, A. K. Sinha, and R. Singh, Phys. Rev. C **81**, 044610 (2010).

[5] N. Keeley, J. S. Lilley, J. X. Wei, M. Dasgupta, D. J. Hinde, J. R. Leigh, J. C. Mein, C. R. Morton, H. Timmers, and N. Rowley, Nucl. Phys. A **628**, 1 (1998).

[6] K. Hagino and N. Takigawa, Prog. Theor. Phys. **128**, 1061 (2012).

[7] C. J. Lin, H. M. Jia, H. Q. Zhang, X. X. Xu, F. Yang, L. Yang, P. F. Bao, L. J. Sun, and Z. H. Liu, EPJ Web Conf. **63**, 02007 (2013).

[8] Khushboo, S. Mandal, N. Madhavan, S. Muralithar, J. J. Das, S. Nath, A. Jhingan, J. Gehlot, B. Behera, S. Verma, H. Singh, S. Kalkal, and R. Singh, EPJ Web Conf. **163**, 00029 (2017), and the references therein.

[9] R. A. Broglia, C. H. Dasso, S. Landowne, and A. Winther, Phys. Rev. C **27**, 2433 (1983).

[10] M. Trotta, A.M. Stefanini, L. Corradi, A. Gadea, F. Scarlassara, S. Beghini, and G. Montagnoli, Phys. Rev. C **65**, 011601(R) (2001).

[11] G. Montagnoli, A. M. Stefanini, C. L. Jiang, H. Esbensen, L. Corradi, S. Courtin, E. Fioretto, A. Goasduff, F. Haas, A. F. Kifle, C. Michelagnoli, D. Montanari, T. Mijatovic, K. E. Rehm, R. Silvestri, P. P. Singh, F. Scarlassara, S. Szilner, X. D. Tang, and C. A. Ur, Phys. Rev. C **85**, 024607 (2012).

[12] G. L. Zhang, X. X. Liu, and C. J. Lin, Phys. Rev. C **89**, 054602 (2014).

[13] A. M. Stefanini, G. Montagnoli, F. Scarlassara, C. L. Jiang, H. Esbensen, E. Fioretto, L. Corradi, B. B. Back, C. M. Deibel, B. Di Giovine, J. P. Greene, H. D. Henderson, S. T. Marley, M. Notani, N. Patel, K. E. Rehm, D. Sewerinyak, X. D. Tang, C. Ugalde, and S. Zhu, Eur. Phys. J. A **49**, 63 (2013).

[14] H. M. Jia, C. J. Lin, F. Yang, X. X. Xu, H. Q. Zhang, Z. H. Liu, L. Yang, S. T. Zhang, P. F. Bao, and L. J. Sun, Phys. Rev. C **86**, 044621 (2012).

[15] M. Beckerman, M. Salomaa, A. Sperduto, H. Enge, J. Ball, A. DiRienzo, S. Gazes, Y. Chen, J. D. Molitoris, and Mao Naifeng, Phys. Rev. Lett. **45**, 1472 (1980).

[16] V. Tripathi, L. T. Baby, J. J. Das, P. Sugathan, N. Madhavan, A. K. Sinha, P. V. MadhusudhanaRao, S. K. Hui, R. Singh, and K. Hagino, Phys. Rev. C **65**, 014614 (2001).

[17] H. Timmers, D. Ackermann, S. Beghini, L. Corradi, J. H. He, G. Montagnoli, F. Scarlassara, A. M. Stefanini, and N. Rowley, Nucl. Phys. A **633**, 421 (1998).

[18] H. Timmers, L. Corradi, A. M. Stefanini, D. Ackermann, J. H. He, S. Beghini, G. Montagnoli, F. Scarlassara, G. F. Segato, and N. Rowley, Phys. Lett. B **399**, 35 (1997).

[19] A. M. Stefanini, L. Corradi, A. M. Vinodkumar, Y. Feng, F. Scarlassara, G. Montagnoli, S. Beghini, and M. Bisogno, Phys. Rev. C **62**, 014601 (2000).

[20] A. A. Sonzogni, J. D. Bierman, M. P. Kelly, J. P. Lestone, J. F. Liang, and R. Vandenbosch, Phys. Rev. C **57**, 722 (1998).

[21] J. F. Liang, L. L. Lee, J. C. Mahon, and R. J. Vojtech, Phys. Rev. C **50**, 1550 (1994), and references therein.

[22] H. A. Aljuwair, R. J. Ledoux, M. Beckerman, S. B. Gazes, J. Wiggins, E. R. Cosman, R. R. Betts, S. Saini, and O. Hansen, Phys. Rev. C **30**, 1223 (1984).

[23] A. M. Stefanini, B. R. Behera, S. Beghini, L. Corradi, E. Fioretto, A. Gadea, G. Montagnoli, N. Rowley, F. Scarlassara, S. Szilner, and M. Trotta, Phys. Rev. C **76**, 014610 (2007).

[24] H. Q. Zhang, C. J. Lin, F. Yang, H. M. Jia, X. X. Xu, Z. D. Wu, F. Jia, S. T. Zhang, Z. H. Liu, A. Richard, and C. Beck, Phys. Rev. C **82**, 054609 (2010).

[25] H. M. Jia, C. J. Lin, F. Yang, X. Xu, H. Q. Zhang, Z. H. Liu, Z. D. Wu, L. Yang, N. R. Ma, P. F. Bao, and L. J. Sun, Phys. Rev. C **89**, 064605 (2014).

[26] H. M. Jia, C. J. Lin, L. Yang, X. X. Xu, N. R. Ma, L. J. Sun, F. Yang, Z. D. Wu, H. Q. Zhang, Z. H. Liu, and D. X. Wang, Phys. Lett. B **755**, 43 (2016).

[27] A. M. Stefanini, F. Scarlassara, S. Beghini, G. Montagnoli, R. Silvestri, M. Trotta, B. R. Behera, L. Corradi, E. Fioretto, A. Gadea, Y. W. Wu, S. Szilner, H. Q. Zhang, Z. H. Liu, M. Ruan, F. Yang, and N. Rowley, Phys. Rev. C **73**, 034606 (2006).

[28] A. M. Stefanini, G. Montagnoli, M. DelFabbro, G. Colucci, P. Colovic, L. Corradi, E. Fioretto, F. Galtarossa, A. Goasduff, J. Grebosz, M. Heine, G. Jaworski, M. Mazzocco, T. Mijatovic, S. Szilner, M. Bajzek, D. Brugnara, M. Siciliano, and I. Zanon, Phys. Rev. C **100**, 044619 (2019).

[29] S. Biswas, A. Chakraborty, A. Jhingan, D. Arora, B. R. Behera, R. Biswas, N. K. Deb, S. S. Ghugre, P. K. Giri, K. S. Golda, G. Kaur, A. Kumar, M. Kumar, B. Mukherjee, B. K. Nayak, A. Parihari, N. K. Rai, S. Rai, R. Raut, R. N. Sahoo, and A. K. Sinha, Phys. Rev. C **102**, 014613 (2020).

[30] S. Biswas, A. Chakraborty, A. Jhingan, D. Arora, B. R. Behera, R. Biswas, N. K. Deb, S. S. Ghugre, P. K. Giri, K. S. Golda, G. Kaur, A. Kumar, M. Kumar, B. Mukherjee, B. K. Nayak, A. Parihari, N. K. Rai, S. Rai, R. Raut, R. N. Sahoo, and A. K. Sinha, Ind. Jour. of Pure & App. Phys. **58**, 409 (2020).

[31] N. K. Deb, K. Kalita, H. A. Rashid, S. Nath, J. Gehlot, N. Madhavan, R. Biswas, R. N. Sahoo, P. K. Giri, A. Das, T. Rajbongshi, A. Parihari, N. K. Rai, S. Biswas, Khushboo, A. Mahato, B. J. Roy, A. Vinayak, and A. Rani, Phys. Rev. C **102**, 034603 (2020).

[32] R. N. Sahoo, M. Kaushik, A. Sood, A. Sharma, S. Thakur, P. Kumar, M. M. Shaikh, R. Biswas, A. Yadav, M. K. Sharma, J. Gehlot, S. Nath, N. Madhavan, R. G. Pillay, E. M. Kozulin, G. N. Knyazheva, K. V. Novikov, and P. P. Singh, Phys. Rev. C **102**, 024615 (2020).

[33] R. N. Sahoo, M. Kaushik, A. Sood, P. Kumar, A. Sharma, S. Thakur, P. P. Singh, P. K. Raina, R. Biswas, J. Gehlot, S. Nath, N. Madhavan, A. Yadav, M. Shaikh, M. K. Sharma, N. K. Deb, A. Rani, A. Banerjee, U. Gupta, B. J. Roy, B. P. Singh, and R. Prasad, JPS Conf. Proc. **32**, 010016 (2020).

[34] S. Saha, Y. K. Agarwal, and C. V. K. Baba, Phys. Rev. C **49**, 2578 (1994).

[35] E. Vulgaris, L. Grodzins, S. G. Steadman, and R. Ledoux, Phys. Rev. C **33**, 2017 (1986).

[36] R. Wadsworth, A. Kogan, P. R. G. Lornie, M. R. Nixon, H. G. Price, and P. J. Twin, J. Phys. G: Nucl. Phys. **3**, 35 (1977).

[37] P. Patrawale and R. Kulkarni, J. Phys. G: Nucl. Phys. **3**, 401 (1977).

[38] A. Trzcinska, E. Piasecki, K. Hagino, W. Czarnacki, P. Decowski, N. Keeley, M. Kisielinski, P. Koczon, A. Kordyasz, E. Koshchiy, M. Kowalczyk, B. Lommel, A. Stolarz, I. Strojek, and K. Zerva, Phys. Rev. C **92**, 034619 (2015).

[39] D. Kanjilal, S. Chopra, M. M. Narayanan, I. S. Iyer, V. Jha, R. Joshi, and S. K. Datta, Nucl. Instrum. Methods Phys. Res. A **328**, 97 (1993).

[40] N. K. Deb, K. Kalita, S. R. Abhilash, P. K. Giri, R. Biswas, G. R. Umapathy, D. Kabiraj, and S. Chopra, Vacuum **163**, 148 (2019).

[41] N. K. Deb, K. Kalita, P. K. Giri, S. R. Abhilash, G. R. Umapathy, R. Biswas, A. Das, D. Kabiraj, S. Chopra, and M. Bhuyan, J. Radioanal. Nucl. Chem. **326**, 97 (2020).

[42] A. K. Sinha, N. Madhavan, J. J. Das, P. Sugathan, D. O. Kataria, A. P. Patro, and G. K. Mehta, Nucl. Instrum. Methods Phys. Res., Sect. A **339**, 543 (1994).

[43] A. Gavron, Phys. Rev. C **21**, 230 (1980).

[44] B. P. Ajith Kumar, E. T. Subramaniam, K. Singh, and R. K. Bowmik, FREEDOM, high speed DAS, SANAI, Trombay, India, 1997, see also http://www.iuac.res.in/elab/das/ppdas/Tutorials/fuman.html.

[45] E. T. Subramaniam, B. P. Ajith Kumar, and R. K. Bowmik, Collection and Analysis of Nuclear Data using Linux nEtwork (unpublished).

[46] R. Brun and F. Rademakers, Nucl. Instrum. Methods Phys. Res. A **389**, 81 (1997).

[47] R. N. Sahoo, M. Kaushik, A. Sood, P. Kumar, A. Sharma, S. Thakur, P. P. Singh, P. K. Raina, M. M. Shaikh, R. Biswas, A. Yadav, J. Gehlot, S. Nath, N. Madhavan, V. Srivastava, M. K. Sharma, B. P. Singh, R. Prasad, A. Rani, A. Banerjee, U. Gupta, N. K. Deb, and B. J. Roy, Phys. Rev. C **99**, 024607 (2019).

[48] T. Rajbongshi, K. Kalita, S. Nath, J. Gehlot, T. Banerjee, I. Mukul, R. Dubey, N. Madhavan, C. J. Lin, A. Shamlath, P. V. Laveen, M. Shareef, N. Kumar, P. Jisha, and P. Sharma, Phys. Rev. C **93**, 054622 (2016).

[49] S. Nath, P. V. Rao, S. Pal, J. Gehlot, E. Prasad, G. Mohanto, S. Kalkal, J. Sadhukhan, P. D. Shidling, K. S. Golda, A. Jhingan,

N. Madhavan, S. Muralithar, and A. K. Sinha, Phys. Rev. C **81**, 064601 (2010); S. Nath, J. Gehlot, E. Prasad, J. Sadhukhan, P. D. Shidling, N. Madhavan, S. Muralithar, K. S. Golda, A. Jhingan, T. Varughese, P. V. Rao, A. K. Sinha, and S. Pal, Nucl. Phys. A **850**, 22 (2011).

[50] S. Nath, Comput. Phys. Commun. **180**, 2392 (2009).

[51] K. Hagino, N. Rowley, and T. Kruppa, Comput. Phys. Commun. **123**, 143 (1999).

[52] R. A. Broglia and A. Winther, *Heavy ion Reaction Lecture Notes, Vol. 1: Elastic and Inelastic Reactions* (Benjamin/Cummings, Reading, MA, 1981).

[53] O. Akyüz, and A. Winther, in Nuclear Structure and Heavy-ion Reactions, *Proceedings of the International School of Physics Enrico Fermi, Course LXXVII, Varenna*, edited by R. A. Broglia *et al.* (North Holland, Amsterdam, 1981).

[54] C. L. Jiang, K. E. Rehm, B. B. Back, H. Esbensen, R. V. F. Janssens, A. M. Stefanini, and G. Montagnoli, Phys. Rev. C **89**, 051603(R) (2014).

[55] E. Piasecki, M. Kowalczyk, S. Yusa, A. Trzcinska, and K. Hagino, Phys. Rev. C **100**, 014616 (2019)

[56] N. Rowley, G. R. Satchler, and P. H. Stelson, Phys. Lett. B **254**, 25 (1991).

[57] N. Rowley, Nucl. Phys. A **538**, 205 (1992).

[58] M. Beckerman, J. Ball, H. Enge, M. Salomaa, A. Sperduto, S. Gazes, A. DiRienzo, and J. D. Molitoris, Phys. Rev. C **23**, 1581 (1981).

[59] A. M. Borges, C. P. daSilva, D. Pereira, L. C. Chamon, E. S. Rossi, and C. E. Aguiar, Phys. Rev. C **46**, 2360 (1992).

[60] C. P. Silva, D. Pereira, L. C. Chamon, E. S. Rossi, G. Ramirez, A. M. Borges, and C. E. Aguiar, Phys. Rev. C **55**, 3155 (1997).